

Non-equilibrium ideal-gas dissociation after a curved shock wave

By H. G. HORNUNG

Department of Physics, Australian National University, Canberra

(Received 2 December 1974 and in revised form 30 September 1975)

Analytic solutions are obtained for non-equilibrium dissociating flow of an inviscid Lighthill–Freeman gas after a curved shock, by dividing the flow into a thin reacting layer near the shock and a frozen region further downstream. The method of matched asymptotic expansions is used, with the product of shock curvature and reaction length as the small parameter. In particular, the solution gives expressions for the reacting-layer thickness, the frozen dissociation level, effective shock values of the frozen flow and the maximum density on a streamline as functions of free-stream, gas and shock parameters. Numerical examples are presented and the results are compared with experiments.

1. Introduction

This paper is concerned with inviscid, adiabatic, hypersonic flow of a diatomic gas after a curved shock wave under conditions where the free-stream speed V'_∞ is sufficiently high for the gas to be heated to a post-shock temperature at which it will dissociate. A Lighthill–Freeman ideal gas is considered, for which the reaction rate is given by (see Freeman 1958)

$$\frac{d\alpha}{dt'} = C' \rho' T'^{\eta} \left\{ (1 - \alpha) \exp\left(-\frac{\theta'_a}{T'}\right) - \alpha^2 \frac{\rho'}{\rho'_a} \right\}, \quad (1.1)$$

where t' , ρ' , T' and α are time, density, temperature and dissociation fraction, and C' , η , θ'_a and ρ'_a are constants describing the rate and equilibrium properties of the gas. It is assumed that the dissociation rate near the shock is large, that is

$$\frac{C' \rho' T_s'^{\eta} \exp(-\theta'_a/T_s')}{V'_\infty k'_0} \gg 1, \quad (1.2)$$

where $1/k'_0$ is a typical length scale, e.g. the radius of curvature of the shock. The recombination rate is assumed to be negligible throughout the flow. This condition may be written as

$$C' \rho'^2 T'^{\eta} \alpha^2 / \rho'_a V'_\infty k'_0 \ll 1 \quad (1.3)$$

whenever the time available for recombination may be represented by $(V'_\infty k'_0)^{-1}$. This is not permissible in the vicinity of a stagnation point. However, the distance from a stagnation point where the flow speed becomes so small that the recombination rate becomes significant can be shown to be of order

$$\Delta' \exp(-V'_\infty \rho'_a k'_0 / C' \rho'^2 T'^{\eta} \alpha^2),$$

where Δ' is the distance from the shock wave to the stagnation point. Since the argument of the exponential is a large negative number, only an exponentially small region has to be excluded from the flow field considered in order to justify the neglect of recombination throughout the remainder.

A further simplification of the rate equation is afforded by the fact that, for situations where dissociation is important in gases such as nitrogen or oxygen, T' is much smaller than θ'_d , so that the temperature dependence of the dissociation rate is very strongly dominated by the exponential function, and the factor $C'\rho'T'^n(1-\alpha)$ may be considered constant (see also Freeman 1958). With the above approximations, the reaction-rate equation is written as

$$\frac{d\alpha}{dt'} = \frac{V'_\infty k'_0}{\epsilon} \exp\left(-\frac{\theta'_d}{T'}\right), \quad (1.4)$$

where ϵ is a small constant parameter. In the experimental nitrogen flow to be considered below, the left-hand side of (1.2) is $\simeq 30$, the left-hand side of (1.3) is $\simeq 10^{-3}$ and $\epsilon \simeq 10^{-5}$.

Using the dissociation model (1.4) it is possible to form a qualitative picture of the processes occurring along a streamline after it crosses a curved shock. As dissociation proceeds, the temperature falls. As a result the dissociation rate soon becomes so small as to be negligible compared with $k'_0 V'_\infty$; that is, no significant further dissociation occurs over a length scale $1/k'_0$. If the temperature is also lowered by an agency other than the dissociation, the point where no significant further dissociation occurs is moved closer to the shock. In the situation of interest here the additional temperature-lowering agency is the negative pressure gradient associated with the shock curvature.

The flow may thus be divided into a region near the shock in which strong dissociation occurs, the thickness of which depends on ϵ and the shock curvature, and a region further downstream in which no significant dissociation or recombination occurs, that is a frozen region. Of particular interest is the variation of the thickness of the reacting layer, and of the frozen dissociation level, with shock shape and free-stream conditions. In addition, the effective shock conditions for the frozen flow downstream of the reacting layer are to be found.

The idea that the flow after a curved shock may be divided into a reacting region close to the shock and a frozen region further downstream is not new. It was suggested in the conclusions of Hornung (1972) that such a division might lead to a sufficiently simple problem to be capable of solution by matched asymptotic expansions, on the basis of the qualitative pattern exhibited by experimental results on blunt-body flows. Also, Stalker (1972, private communication) recognized that the freezing of the flow occurs because of the strong exponential temperature dependence of the reaction rate and the effect of a pressure gradient on temperature. This led to an approximate analysis of the problem by Furler (1973). The present work has benefited greatly from ideas raised in discussions with Stalker and Furler.

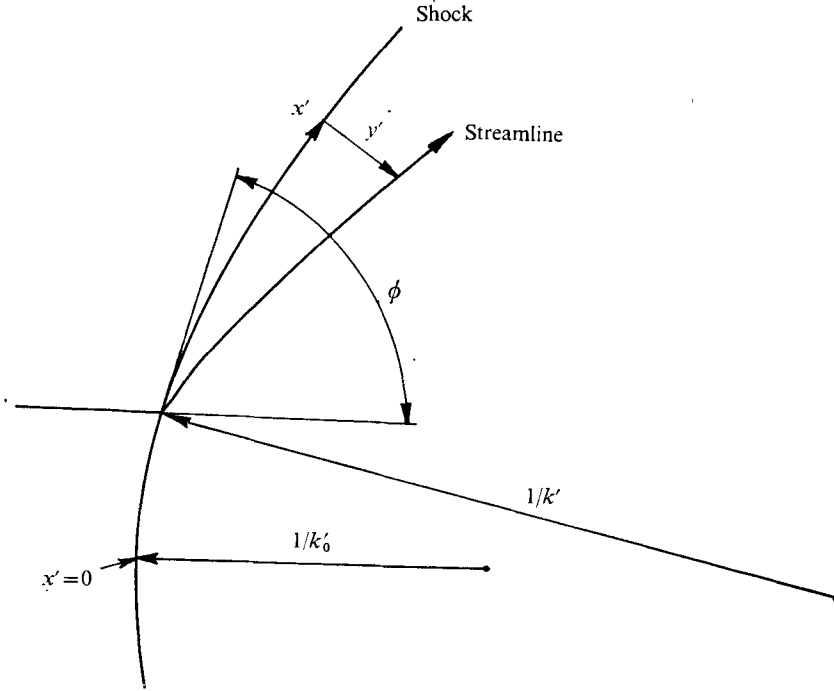


FIGURE 1. Notation.

2. Equations of motion on a streamline

The main purpose of this section is to obtain an expression for the pressure gradient along a streamline behind a curved shock. In obtaining this expression, which is needed for the next section, some features of reacting flow after a curved shock may be demonstrated conveniently.

Take x' and y' as co-ordinates parallel and perpendicular to a shock of curvature $k'(x')$ and making an angle $\phi(x')$ with the direction of the uniform free stream, of velocity V'_∞ (see figure 1). k' is taken to be positive if the shock is convex towards the upstream direction. Let u' and v' be the components of velocity in the x' and y' directions respectively, p' and ρ' be the pressure and density, and h' be the specific enthalpy of the gas. Scale the variables according to

$$\left. \begin{aligned} h &= h'/(V'_\infty)^2, & p &= p'/\rho_\infty(V'_\infty)^2, & v &= v'/V'_\infty, & u &= u'/V'_\infty, \\ \rho &= \rho'/\rho'_\infty, & x &= x'k'_0, & y &= y'k'_0, & k &= k'/k'_0, \end{aligned} \right\} \quad (2.1)$$

where the subscript ∞ refers to conditions in the free stream and k'_0 is the shock curvature at a representative point. Introducing a non-equilibrium variable α (e.g. the dissociation fraction), the caloric equation of state is of the form

$$h = h(p, \rho, \alpha). \quad (2.2)$$

The conservation equations for momentum, energy and mass are (see Hayes & Probstein 1966, p. 267)

$$\left. \begin{aligned} uu_x + (1 - ky)vu_y - kw + p_x/\rho &= 0, \\ uv_x + (1 - ky)vv_y + ku^2 + (1 - ky)p_y/\rho &= 0, \\ h_p p_y + h_\rho \rho_y + h_\alpha \alpha_y + vv_y + uu_y &= 0, \\ (\rho u)_x - k\rho v + (1 - ky)(\rho v)_y &= 0. \end{aligned} \right\} \quad (2.3)$$

The subscripts denote partial differentiation. The energy equation has been differentiated with respect to y . Differentiating it with respect to x yields an expression for ρ_x , which will be used in the continuity equation later:

$$\rho_x = -\{wu_x + vv_x + h_p p_x + h_\alpha \alpha_x\}/h_\rho. \quad (2.4)$$

A thermal equation of state

$$T = T(p, \rho, \alpha) \quad (2.5)$$

is also required, because the reaction rate is usually specified in terms of the temperature $T' = T(V'_\infty)^2/R'$, where R' is the specific gas constant:

$$\frac{d\alpha}{dt} = \frac{d\alpha}{dt}(T, \rho, \alpha). \quad (2.6)$$

The derivative with respect to time ($t = t' V'_\infty k'_0$, with origin at the shock) is understood to be taken along a streamline (substantial derivative).

The boundary conditions at the shock are (see Vincenti & Kruger 1965, p. 180)

$$\left. \begin{aligned} p_1 - p_\infty &= m^2(1 - \rho_1^{-1}), & \alpha_1 &= \alpha_\infty, & v_1 &= m/\rho_1, \\ h_1 - h_\infty &= \frac{1}{2}m^2(1 - \rho_1^{-2}), & u_1^2 &= 1 - m^2, \end{aligned} \right\} \quad (2.7)$$

where $m = \sin \phi$ and the subscript 1 denotes values just downstream of the shock. ρ_1 can be obtained with a suitable model for (2.2) from (2.7).

If the problem is posed in this fashion, that is, specifying boundary conditions only on the shock, only supersonic post-shock flows can strictly be determined. However, experience with inverse numerical techniques applied to blunt-body problems shows that, over a distance which is small compared with the radius of curvature of the shock, the shock boundary conditions are sufficient, for practical purposes, to specify the problem.

By setting k and the x derivatives equal to zero in (2.3) a partial solution may be obtained for a straight shock:

$$p - p_\infty = m^2(1 - \rho^{-1}), \quad v = m/\rho, \quad u^2 = 1 - m^2, \quad (2.8a-c)$$

$$\frac{m^3}{\rho^3} \rho_y = \frac{h_\alpha d\alpha/dt}{\rho^{-1} - \rho^2 m^{-2} h_\rho - h_p}, \quad \alpha_y = \frac{\rho}{m} \frac{d\alpha}{dt}. \quad (2.8d, e)$$

With suitable models for (2.2), (2.5) and (2.6), (2.8d, e) may be integrated. This solution is, of course, precisely that for a normal shock ($m = 1$) with a superimposed constant transverse velocity u .

Returning to the curved shock, (2.3) may be solved for the y derivatives of p , ρ , v and u explicitly, retaining α_y as a parameter:

$$p_y F = \rho h_\alpha \alpha_y - k\rho \left\{ u \left(1 - \frac{\rho h_\rho}{v^2} \right) \left(\frac{v_x}{k} + u \right) + \frac{u}{v} E + \rho \frac{h_\rho}{v} \left(\frac{(\rho u)_x}{\rho k} - v \right) \right\} / (1 - ky), \quad (2.9a)$$

$$u_y = -kv^{-1}E/(1 - ky), \quad (2.9b)$$

$$vv_y F = -h_\alpha \alpha_y + k \left\{ \rho u h_\rho \left(\frac{v_x}{k} + u \right) + \frac{u}{v} E + \rho \frac{h_\rho}{v} \left(\frac{(\rho u)_x}{\rho k} - v \right) \right\} / (1 - ky), \quad (2.9c)$$

$$\rho_y F = \frac{\rho h_\alpha \alpha_y}{v^2} - \frac{k\rho}{v^2} \left\{ \rho u h_p \left(\frac{v_x}{k} + u \right) + \frac{u}{v} E + (1 - \rho h_p) \left(\frac{(\rho u)_x}{\rho k} - v \right) \right\} / (1 - ky), \quad (2.9d)$$

where
$$E = \frac{p_x}{\rho k} + u \frac{u_x}{k} - uv, \quad F = 1 - \rho \left(\frac{h_p}{v^2} + h_p \right). \quad (2.10)$$

By combining x and y derivatives according to

$$\frac{d}{dt} = v \frac{\partial}{\partial y} + \frac{u}{1 - ky} \frac{\partial}{\partial x}$$

and using (2.4), the time derivatives of p , ρ and V become

$$F \frac{dp}{dt} = \rho h_\alpha \frac{d\alpha}{dt} + k \frac{\rho^2 h_p}{v} G, \quad (2.11 a)$$

$$F \frac{d\rho}{dt} = \frac{\rho}{v^2} h_\alpha \frac{d\alpha}{dt} - k \frac{\rho^2}{v} \left(h_p - \frac{1}{\rho} \right) G, \quad (2.11 b)$$

$$V \frac{dV}{dt} = - \frac{1}{\rho} \frac{dp}{dt}, \quad (2.11 c)$$

where $V = (u^2 + v^2)^{1/2}$ is the flow speed and

$$G = \left\{ v^2 + u^2 + \frac{uv_x}{k} - \frac{u}{v} \frac{1}{\rho} \frac{p_x}{k} - v \frac{u_x}{k} \right\} / (1 - ky). \quad (2.12)$$

3. The differential equation for $\alpha(T)$ along a streamline

Differentiating (2.5) with respect to t , substituting for the time derivatives of p and ρ from (2.11) and dividing by $d\alpha/dt$ results in the following equation:

$$F \frac{dT}{d\alpha} = \left(\frac{T_\rho}{v^2} + T_p \right) \rho h_\alpha + FT_\alpha + \frac{k\rho^2 G}{v} \left[T_p h_p - T_\rho \left(h_p - \frac{1}{\rho} \right) \right] \frac{dt}{d\alpha}. \quad (3.1)$$

In this section (3.1) is simplified by introducing models for the rate and thermodynamics of the gas and making the assumptions discussed in the introduction. An ideal dissociating gas is considered (Lighthill 1957; Freeman 1958), for which (2.2), (2.5) and (2.6) become

$$h = \frac{4 + \alpha}{1 + \alpha} \frac{p}{\rho} + \alpha\theta, \quad T = \frac{p}{\rho(1 + \alpha)}, \quad \frac{d\alpha}{dt} = \frac{1}{\epsilon} e^{-\theta/T}. \quad (3.2)$$

θ is the dissociation energy $R'\theta'_d$ per unit mass normalized by $V_\infty'^2$ and is $O(1)$ for situations where dissociation produces significant effects. The relevant derivatives of T and h may now be substituted into (3.1), which becomes

$$\frac{dT}{d\alpha} = \frac{(1 - \rho v^2/p)\theta + T + \epsilon kvG e^{\theta/T}}{(4 + \alpha) \left(1 - \frac{3}{4 + \alpha} \frac{\rho v^2}{p} \right)}. \quad (3.3)$$

Near the shock, where T is relatively large, the term in ϵ is small, and the straight-shock solution (2.8) is recovered. Further downstream, where the temperature has fallen to a sufficiently low value, the exponential term becomes large, and the term in ϵ eventually becomes $O(1)$. Let this region be called the transition region. It is necessary to estimate the order of magnitude of the various terms of (3.3)

in the transition region. This may be done by evaluating the straight-shock solution (which applies for $yk \ll 1$) in the transition region, defined by

$$\epsilon kvGe^{\theta/T} = O(1). \quad (3.4)$$

Since the flow is hypersonic, p_∞ may be neglected in (2.8), so that near the shock

$$p/\rho v^2 = \rho - 1. \quad (3.5)$$

Together with (3.2) this yields

$$\frac{\rho v^2}{p} = \frac{T(1+\alpha)}{m^2} \left(1 - \frac{1}{\rho}\right)^{-2}. \quad (3.6)$$

It is clear from (3.4) that T will be $o(1)$ in the transition region. Equations (3.6) and (3.5) show that $\rho v^2/p$ and ρ^{-1} are of the same order as T . Hence $v = m/\rho$ is also of the same order as T in the transition region. Let $T = O[\delta(\epsilon)]$ in the transition region. Equation (3.4) then requires that

$$\epsilon \delta e^{\theta/T} = O(1), \quad \text{or} \quad \theta/T = O(\log(\epsilon \delta)^{-1}) \quad (3.7)$$

in the transition region, so that $\delta = O(1/\log \epsilon^{-1})$, provided that G remains $O(1)$.

It is now necessary to examine the variation of G along a streamline in some detail. To do this, consider first the value of G for a straight shock, $G|_{k=0}$. While the x derivatives in (2.12) are zero in that case, they are all divided by k , and terms such as p_x/k are finite and constant. For a hypersonic straight shock $G|_{k=0}$ may be expressed in terms of ρ and m [see (2.8)]:

$$G|_{k=0} = [3(1-m^2) - m^2/\rho](1-\rho^{-1}). \quad (3.8)$$

However, G deviates from this value when k is not zero. To account for this deviation, write

$$G = G|_{k=0} + y[\partial G_f/\partial y]_1 + \dots \quad (3.9)$$

for small y , where G_f is the frozen value of G ($\alpha_y = 0$) for a curved shock. Differentiating (2.12) with respect to y , substituting from (2.9) and its x derivatives into the resulting equation and retaining only the largest power of ρ_1 gives

$$\left(\frac{\partial G_f}{\partial y}\right)_1 = \frac{\rho_1 k}{4} \left[\frac{7}{2} + \frac{5}{m^2} (1-m^2)^4 + \frac{3}{m} (1-m^2)^2 \right]. \quad (3.10)$$

An estimate of the order of magnitude of the distance y_T of the transition region from the shock may be obtained by writing

$$\frac{dy}{dT} \simeq v_1 \frac{dt}{d\alpha} \frac{d\alpha}{dT} \simeq -\frac{4v_1}{\theta} \epsilon e^{\theta/T}$$

near the shock, $d\alpha/dT$ being taken as constant and equal to its approximate shock value for the purposes of this estimate [see (3.3)]. Substituting $z = \theta/T$ and integrating,

$$y_T \simeq 4\epsilon v_1 \int_{\theta/T_1}^{\log(\epsilon \delta)^{-1}} \frac{e^z}{z^2} dz.$$

For gases like nitrogen, oxygen and carbon monoxide the temperatures at which dissociation is important are such that $\theta/T_1 > 8$; also $\log(\epsilon \delta)^{-1} \gg 1$. The integral

may therefore be approximated by its asymptotic form for large z (the leading term of which is just the integrand), so that, neglecting terms $O(\epsilon)$ and $O(\delta^3)$, $y_T \simeq 4\epsilon\delta^2 v_1 / \theta^2 \epsilon \delta = 4\delta m / \theta^2 \rho_1$. With this result, (3.9) and (3.10) give the order of magnitude of the change $y_T(\partial G_f / \partial y)_1$ in G from the shock to the transition region owing to the shock curvature as $O(\rho_1 y_T) = O(\delta)$, so that

$$G = G|_{k=0} + O(\delta).$$

In the transition region $\rho = O(\delta^{-1})$, however, and (3.8) gives

$$G = 3(1 - m^2) + O(\delta). \tag{3.11}$$

Since the term in G in (3.3) only begins to contribute significantly in the transition region, (3.11) is an adequate representation of G in (3.3), which may now be rewritten in terms of α and T as

$$\frac{dT}{d\alpha} = - \frac{\theta - T\{(1 + \alpha)\theta/m^2 - 1 + O(\delta)\} + 3\epsilon km^{-1}(1 - m^2)(1 + \alpha)Te^{\theta/T}[1 + O(\delta)]}{(4 + \alpha)\left\{1 - \frac{3(1 + \alpha)T}{(4 + \alpha)m^2}[1 + O(\delta)]\right\}}. \tag{3.12}$$

In the transition region, T is itself $O(\delta)$, so that the contribution of the terms labelled $O(\delta)$ in (3.12) is only $O(\delta^2)$. Only a first-order transition solution will be sought below, and these terms become unimportant. Neglecting them and writing

$$b = 3(1 - m^2)km\tau^{-1} \tag{3.13}$$

yields

$$\frac{dT}{d\alpha} = - \frac{\theta - T\{(1 + \alpha)\theta/m^2 - 1\} + b\epsilon(1 + \alpha)Te^{\theta/T}}{(4 + \alpha)\left\{1 - \frac{3(1 + \alpha)T}{4 + \alpha} \frac{T}{m^2}\right\}}. \tag{3.14}$$

The method of solution used in the next section could be applied to (3.14) with success, but since all the features of the solution can be demonstrated with less complexity and good accuracy if α is neglected compared with 1 in the two terms in curly brackets in (3.14), the equation

$$\frac{d\alpha}{d\xi} = - \frac{(4 + \alpha)(1 - \lambda\xi)}{1 - \mu\xi + \epsilon b\xi(1 + \alpha)e^{1/\xi}} \tag{3.15}$$

is taken as the model equation for the flow, where $\xi = T/\theta$ and

$$\mu = (\theta - m^2)/m^2, \quad \lambda = \frac{3}{4}\theta/m^2. \tag{3.16}$$

As the temperature falls with proceeding dissociation, the ϵ term, which is due to the negative pressure gradient accompanying the curved shock, becomes important and finally dominates, when $T = o(\theta/\log(b\epsilon)^{-1})$. $d\alpha/dt$ then approaches zero and

$$\frac{dT}{dt} = \frac{dT}{d\alpha} \frac{d\alpha}{dt} \rightarrow - \frac{1 + \alpha}{4 + \alpha} bT.$$

Since α is constant and equal to α_0 under such conditions, this may be integrated to give the asymptotic frozen-flow result

$$T = T_0 \exp\left(- \frac{1 + \alpha_0}{4 + \alpha_0} bt\right). \tag{3.17}$$

It should be pointed out at this juncture that the change in the character of $dT/d\alpha$ occurs in a different way when $d\alpha/dt$ does not change so rapidly with temperature. This may be illustrated conveniently with a gas model such as that of Becker & Böhme (1969):

$$p/\rho = T, \quad h = C_p T + c\alpha, \quad d\alpha/dt = (T - \alpha)/\tau,$$

with the constants C_p , c and τ as in (3.1). The result is

$$\frac{dT}{d\alpha} = \frac{c(1 - \rho v^2/p) + b\tau(1 + \alpha)(T - \alpha)^{-1}}{C_p - (C_p - 1)\rho v^2/p}.$$

As the relaxation proceeds, α increases and T falls, but $T - \alpha$ then changes sign, so that α finally approaches the still falling T (i.e. approaches equilibrium) from above, and the c term becomes unimportant. Note that this difference between this equation and (3.3) arises from the more gently varying rate as compared with (3.2).

4. Solution for $\alpha(t)$ along a streamline

In this section a solution of (3.15) is obtained with the boundary condition

$$\alpha = 0 \quad \text{at} \quad \xi = \xi_1 = 6m^2/49\theta, \quad (4.1)$$

in $\xi \leq \xi_1$ and with $\epsilon \ll 1$. Note that m is a constant for each streamline, being the value of $\sin \phi$ at the point where that particular streamline crossed the shock. Consider first the region close to the shock. Expand α in the form

$$\alpha(\xi, \epsilon) = \alpha_R^{(1)}(\xi) + \epsilon \alpha_R^{(2)}(\xi) + \dots, \quad (4.2)$$

where the subscript R signifies relevance to the reacting layer. The second term in this expansion has to be considered because it is the source of terms which become significant in the transition region, while the terms $O(\delta)$ neglected in the derivation of (3.15) decrease to even smaller significance in the transition region. Substituting (4.2) into (3.15), collecting terms of equal order and solving for $\alpha_R^{(1)}$ and $\alpha_R^{(2)}$ with $\alpha_R^{(2)}(\xi_1) = 0$ gives

$$\alpha_R(\xi, \epsilon) = 4 \left[\frac{A_1}{A(\xi)} - 1 \right] + 4\epsilon b \frac{A_1}{A(\xi)} \int_{\xi_1}^{\xi} \frac{z e^{1/z} (1 - \lambda z)}{(1 - \mu z)^2} \left[\frac{4A_1}{A(z)} - 3 \right] dz, \quad (4.3)$$

where

$$A(\xi) = \exp(\lambda \mu^{-1} \xi) (1 - \mu \xi)^{-\mu^{-1}(1 - \lambda/\mu)} \\ \simeq 1 + \xi + \frac{1}{6} \lambda \xi^2 + O(\xi^3), \quad (4.4)$$

and the values of λ and μ in (3.14) are used to simplify $1 + \mu - \lambda$ to $\frac{1}{3}\lambda$. The constant $A_1 = A(\xi_1)$. When

$$\xi \simeq 1/\{\log [(b\epsilon)^{-1} \log (b\epsilon)^{-1}]\}, \quad (4.5)$$

the ϵ term in (3.15) becomes $O(1)$. Introduce a new independent variable

$$\tilde{\xi} = \left[\xi - \frac{1}{\log (b\epsilon\delta)^{-1}} \right] \delta^{-2} \quad (4.6)$$

for the region in which $\tilde{\xi} = O(1)$, δ being defined by

$$\delta = 1/\log (b\epsilon)^{-1}. \quad (4.7)$$

Writing (3.15) in terms of $\tilde{\xi}$ for the transition region yields

$$\frac{d\alpha_T}{d\tilde{\xi}} = \frac{-(4 + \alpha_T)\delta^2}{1 + (1 + \alpha_T)e^{-\tilde{\xi}}[1 + (1 + 2\tilde{\xi})\delta \log \delta]} + O(\delta^3), \quad (4.8)$$

the terms in λ and μ having disappeared into the higher-order terms. To solve (4.8), write

$$\alpha_T(\tilde{\xi}, \delta) = C_0 + C_1\delta + C_2\delta^2 \log \delta + \alpha_T^{(3)}(\tilde{\xi})\delta^2 + o(\delta^2) \quad (4.9)$$

and substitute into (4.8). A simple equation for $\alpha_T^{(3)}$ results:

$$\frac{d\alpha_T^{(3)}}{d\tilde{\xi}} = -\frac{4 + C_0}{1 + (1 + C_0)e^{-\tilde{\xi}}}, \quad (4.10)$$

giving

$$\alpha_T(\tilde{\xi}, \delta) = C_0 + C_1\delta + C_2\delta^2 \log \delta + \{C_3 - (4 + C_0)[\tilde{\xi} + \log(1 + (1 + C_0)e^{-\tilde{\xi}})]\}\delta^2. \quad (4.11)$$

The C 's are constants which have to be determined by matching $\alpha_R(\xi, \epsilon)$ and $\alpha_T(\xi, \delta)$ term by term in an intermediate region. Choose $\tilde{\xi} = O(1)$ as the matching region, where

$$\tilde{\xi} = \delta^{-2}(\xi - \delta). \quad (4.12)$$

Expressing α_R as a function of $\tilde{\xi}$ and δ in the matching region gives

$$\begin{aligned} \alpha_R(\tilde{\xi}, \delta) = & 4\{A_1[1 - \delta - \delta^2(\frac{1}{8}\lambda + \tilde{\xi}) \\ & + \delta^3((1 - \frac{1}{8}\lambda)\tilde{\xi} + \frac{1}{8}(\mu - \lambda)(3 - 2\mu) - 1) + 4A_1(4A_1 - 3)e^{-\tilde{\xi}}] - 1\} + o(\delta^3). \end{aligned} \quad (4.13)$$

This has to be matched with $\alpha_T(\tilde{\xi}, \delta)$, which may be obtained from (4.6), (4.11) and (4.12) as

$$\begin{aligned} \alpha_T(\tilde{\xi}, \delta) = & C_0 + \delta C_1 + \delta^2 \log \delta (C_2 + 4 + C_0) + \delta^2 [C_3 - (4 + C_0)\tilde{\xi}] \\ & - (4 + C_0)(1 + C_0)\delta^3 e^{-\tilde{\xi}} + o(\delta^3). \end{aligned} \quad (4.14)$$

Equating (4.13) and (4.14) yields

$$C_0 = 4(A_1 - 1), \quad C_1 = -4A_1, \quad C_2 = -(4 + C_0) = -4A_1, \quad C_3 = -\frac{2}{3}A_1\lambda. \quad (4.15)$$

Note that the terms $O(\delta)$ in (3.12) would only appear in the terms $o(\delta^3)$ in (4.13) and (4.14). The transition solution for α becomes

$$\begin{aligned} \alpha_T(\tilde{\xi}, \delta) = & 4(A_1 - 1) \\ & + 4A_1\{-\delta - \delta^2 \log \delta - \delta^2[\frac{1}{8}\lambda - 1 + \tilde{\xi} + \log(1 + [4A_1 - 3]e^{-\tilde{\xi}})]\} + o(\delta^2), \end{aligned} \quad (4.16)$$

which asymptotes for $\tilde{\xi} \rightarrow -\infty$ to the frozen dissociation fraction

$$\alpha_0 = 4A_1\{1 - A_1^{-1} - \delta - \delta^2 \log \delta - \delta^2[\frac{1}{8}\lambda - 1 + \log(4A_1 - 3)]\} + o(\delta^2), \quad (4.17)$$

expressed explicitly in terms of shock shape, free-stream conditions and gas properties.

5. Reacting-layer thickness and effective shock values

The time t for which a particle has travelled along a streamline since crossing the shock may be obtained by integrating

$$\frac{dt}{d\xi} = \frac{dt}{d\alpha} \frac{d\alpha}{d\xi} = \epsilon \exp\left(\frac{1}{\xi}\right) \frac{d\alpha}{d\xi}, \quad (5.1)$$

after substituting for $d\alpha/d\xi$ from (3.15). By finding the forms of the resulting equation in the reacting layer and in the transition region as before, integrating and matching in the intermediate region $\xi = O(1)$, the following result is obtained for t in the transition region:

$$t_T = \frac{4A_1 \delta}{4A_1 - 3} \log [1 + (4A_1 - 3) e^{-\xi}] + o(\delta). \quad (5.2)$$

This confirms the estimate of the order of magnitude of the layer thickness obtained in § 3.

In the region downstream of the reacting layer, the composition on each streamline is frozen at a different value of α_0 , given by (4.17). For the purposes of the frozen region, the thin reacting layer could be regarded as part of the discontinuity at the shock. The effective boundary conditions at this discontinuity may be obtained by extrapolating the frozen behaviour back to $t = 0$. For $t \rightarrow \infty$, that is, for large negative ξ , (5.2) gives

$$\lim_{\xi \rightarrow -\infty} t = \frac{4A_1}{4A_1 - 3} \delta [-\xi + \log(4A_1 - 3)]. \quad (5.3)$$

Writing the asymptotic frozen-flow result (3.17) in terms of ξ and using (4.17) to replace α_0 gives

$$t = \frac{4A_1}{b(4A_1 - 3)} \left\{ [-\log \delta + \log \xi_0 - \delta \log \delta] \left[1 - \frac{3\delta}{4A_1 - 3} \right] - \delta \xi \right\}. \quad (5.4)$$

Comparing (5.3) and (5.4), it can be seen that they give the same result if

$$\xi_0 = \delta \{1 + \delta \log \delta + \delta \log(4A_1 - 3)\} + o(\delta^2). \quad (5.5)$$

Note that this effective shock temperature is almost independent of the actual shock temperature ξ_1 and essentially depends only on δ .

By writing

$$\frac{dp}{d\xi} = \frac{dp}{dt} \frac{dt}{d\alpha} \frac{d\alpha}{d\xi},$$

(2.11) may be used together with the arguments leading to (3.15) to obtain the following equation for the pressure:

$$\frac{1}{\theta} \frac{dp}{d\xi} = - \frac{1 + \alpha - 3\xi - p\theta^{-1}\epsilon b e^{\xi-1}(4 + \alpha)}{1 - \mu\xi + \epsilon b \xi(1 + \alpha) e^{\xi-1}}. \quad (5.6)$$

The same process as was applied to (3.15) in § 4 and to (5.1) may be applied to (5.6) to obtain the transition-layer solution for the pressure:

$$\frac{p_T - p_1}{\theta(4A_1 - 3)} = B_1 - \delta - \frac{4A_1 \delta}{4A_1 - 3} \left[\frac{p_1}{\theta(4A_1 - 3)} + B_1 \right] \log \{1 + (4A_1 - 3) e^{-\xi}\} + o(\delta), \quad (5.7)$$

where

$$B_1 = \frac{\nu}{\mu} \xi_1 - \frac{1-\nu/\mu}{\mu} \log(1-\mu\xi_1) \simeq \xi_1 - \frac{\mu-\nu}{2} \xi_1^2 + O(\xi_1^3) \quad (5.8)$$

and

$$\nu = 3/(4A_1 - 3).$$

Comparison with the frozen-flow solution for p ,

$$p = p_0 e^{-bt}, \quad (5.9)$$

shows the effective shock value of p to be

$$p_0 = p_1 + (4A_1 - 3) \theta [B_1 - \delta]. \quad (5.10)$$

The density in the transition region may now be obtained from (3.2) as

$$\rho = p/\theta\xi(1+\alpha), \quad (5.11)$$

which serves also to determine the effective shock value of the density,

$$\rho_0 = p_0/[\theta\xi_0(1+\alpha_0)].$$

In the frozen limit,

$$\rho = \rho_0 \exp\left(-\frac{3bt}{4+\alpha_0}\right). \quad (5.12)$$

Equation (5.12), like (3.17) and (5.9), corresponds to a flow with a constant ratio of specific heats, equal to $\frac{1}{3}(4+\alpha_0)$, a pressure gradient of $-bp$ and initial conditions $p = p_0$, $T = T_0$ and $\rho = \rho_0$.

6. Numerical example

In this section the nature of the solutions obtained in the previous section is illustrated in the form of numerical examples. It is convenient to test the assumption that λ and μ are independent of α at the same time, by obtaining a numerical solution not of the model equation (3.15), but of (3.14). Similarly the more general forms of (5.1) and (5.6) are integrated. The results are shown as full lines in figure 2 in the form of α , ξ , ρ and p plotted against t for the case $\theta = 0.8$, $m = 0.8$, $\epsilon = 10^{-6}$ and $b = 1.08$. Also shown in the figure are the analytical results. To plot these, α and p are obtained from the transition and frozen solutions [equations (4.16), (5.7) and (5.10)] in terms of $\tilde{\xi}$. $\tilde{\xi}$ is then related to t by the transition and frozen solution for t [equations (5.2), (3.15) and (5.5)]. The density is determined from (5.11). These results are plotted as dotted lines. The frozen solution is continued back to the shock in order to show the quality of the approximation for the effective shock values. In addition, the straight-shock solution ($b = 0$) is superimposed as chain-dotted curves. It may be seen that the actual solution starts in the reacting layer in agreement with the straight-shock solution, departs from it in the transition region and eventually approaches the frozen solution asymptotically. The transition solution is seen to agree with the numerical solution fairly well, discrepancies of up to 3% in ρ and ξ and a discrepancy of about 6% in α_0 being evident. The former are mainly due to the relatively inaccurate result for $t_T(\tilde{\xi})$ given by (5.2), in which only the leading term in an expansion for small ϵ can be retained. The latter is mainly due to neglecting

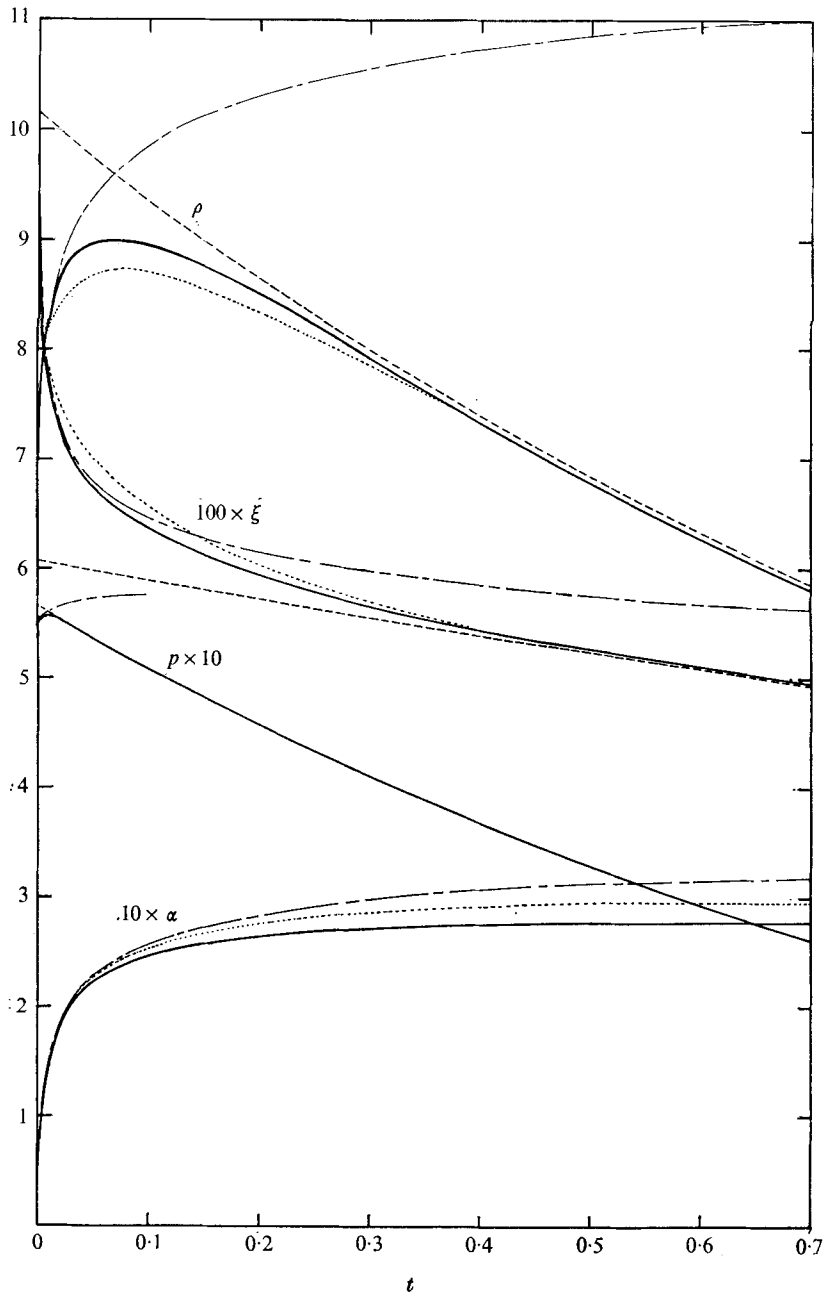


FIGURE 2. Numerical example of flow along a streamline with $\theta = 0.8$, $m = 0.8$, $\epsilon = 10^{-6}$, $b = 1.08$. —, numerical calculation (α dependence of terms represented by λ and μ not neglected); - - - -, frozen solution [equations (3.17), (5.9), (5.12)]; , analytic solution for transition region [equations (4.16), (5.2), (5.7)]; - · - · -, straight-shock solution ($b = 0$).

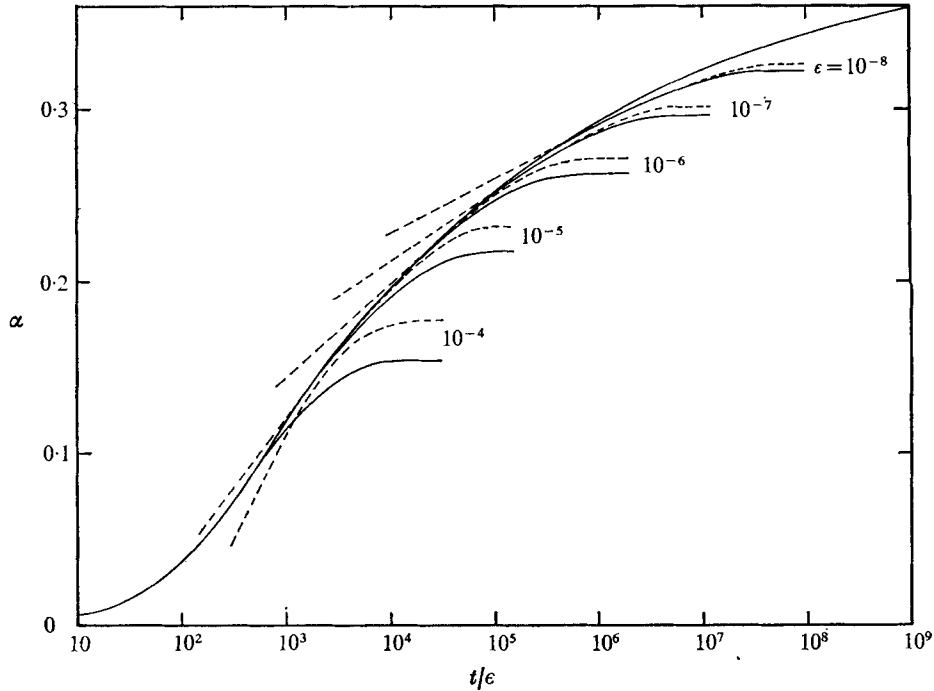


FIGURE 3. Dependence of α on ϵ and t . —, numerical calculation; ---, transition solution [equation (4.16)]. $\theta = 0.6$, $m = 0.8$, $b = 1.08$.

the variation with α of the terms represented by λ and μ . The effect of the reaction on the pressure is shown by the rise in pressure immediately after the shock. As expected, this is quite a small effect. (See also Freeman 1958.) It needs to be included in the analytic solution, however, since its neglect would lead to a doubling of the discrepancy between the density as given by the transition solution and as numerically calculated. The pressure maximum, which coincides with a point of inflexion of the streamline, occurs much earlier than the density maximum on the streamline. At smaller values of θ and for smaller ϵ the effect of the dissociation is larger. Smaller ϵ causes the time to freezing to decrease, but because of its logarithmic dependence on ϵ , a consequence of the form of the temperature dependence of the rate, halving ϵ reduces the time to freezing by only about 10% at $\epsilon \simeq 10^{-6}$.

Because the rate at which α increases in the straight-shock solution becomes very small at large t , the difference between α_T and the straight-shock value is not very significant for t around 0.6. To show that, at large t , α_T does depart from the straight-shock solution, at different points for different values of ϵ , figure 3 shows α plotted against $\log(t/\epsilon)$. Plotted in this form, the straight-shock solution for a particular set of θ , b and m but for all ϵ coincides with that for $\epsilon = 0$. The figure shows the numerical results for $\alpha(t/\epsilon)$ as well as $\alpha_T(t_T/\epsilon)$ with ϵ as a parameter for $\theta = 0.6$, $m = 0.8$ and $b = 1.08$. The straight-shock solution and α_T are seen to merge at about $t = 0.1\epsilon$; as t decreases below about $t = 0.01\epsilon$, in the strongly reacting region, where α_T is no longer valid, they depart from each other

again. The discrepancy between the numerical and analytical value of α_0 arises from considering the terms represented by λ and μ to be independent of α , and from higher-order terms in δ , neglected in (4.17).

7. Position and value of the density maximum: comparison with experiment

The position of the density maximum on a streamline is of interest because density may be measured relatively easily (e.g. by optical interferometry) and because it is quite sensitive to non-equilibrium effects. The maximum may be found by equating the derivative of (5.11) with respect to ξ to zero:

$$\frac{d\rho}{d\xi} = \left[\frac{dp}{d\xi} - \frac{p}{1+\alpha} \frac{d\alpha}{d\xi} - \frac{p}{\xi} \right] / [\theta\xi(1+\alpha)] = 0. \quad (7.1)$$

Expressing the derivatives in terms of α and ξ and solving for ξ gives

$$\xi_* = \left[\log \left(\frac{1}{3\epsilon b} \log \frac{1}{3\epsilon b} \right) \right]^{-1} + o(\delta^2 \log \delta). \quad (7.2)$$

The corresponding value of $\tilde{\xi}$ is

$$\tilde{\xi}_* = \log 3 + O(\delta \log \delta).$$

On substituting $\tilde{\xi} = \tilde{\xi}_*$ in (5.3), the time taken by a particle to traverse the distance from the shock to the density maximum is obtained:

$$t_* = \frac{4A_1 \delta \log \left(\frac{4}{3} A_1 \right)}{(4A_1 - 3)b}. \quad (7.3)$$

The value ρ_* of the density at its peak is then found by putting $\tilde{\xi} = \log 3$ in the transition solutions for p and α and substituting these into (5.11):

$$\rho_* = \frac{1}{\delta} \left[\frac{p_1}{\theta(4A_1 - 3)} + B_1 \right] \left\{ 1 - \delta \log \delta + \delta \left[\frac{4A_1}{4A_1 - 3} \left(1 - \log \frac{4A_1}{3} \right) - \log 3 - \frac{4A_1 - 3}{p_1/\theta + (4A_1 - 3)B_1} \right] \right\}, \quad (7.4)$$

where terms $o(1)$ have been neglected.

In order to convert t_* into the distance to the density maximum, it is necessary to know the behaviour of the flow speed along the streamline. The variation in u from the shock to the transition region may be estimated, from (2.9) and $y_T = O(\delta)$, as $O(\delta k)$. The distance parallel to the shock traversed by a particle from the shock to the density maximum is therefore

$$x_* - x_1 = [u_1 + O(\delta)] t_* = \frac{4A_1 \delta \log \frac{4}{3} A_1}{b(4A_1 - 3)} (1 - m^2)^{\frac{1}{2}} + O(\delta^2). \quad (7.5)$$

The corresponding distance normal to the shock can be expressed as the product of t_* and a suitable average value of the shock normal speed v , namely $2mt_*/(\rho_1 + \rho_*)$:

$$y_* \simeq \frac{8mA_1 \delta \log \frac{4}{3} A_1}{b(\rho_1 + \rho_*)(4A_1 - 3)}. \quad (7.6)$$

To compare the results with experiment, an interferogram of nitrogen flow over a circular cylinder from Hornung (1972) is used. In this flow, the free-stream conditions are $V'_\infty = 5.5 \text{ km/s}$, $\rho'_\infty = 5.5 \times 10^{-6} \text{ g/cm}^3$, $\alpha_\infty = 0.07$, $\theta = 0.92$ and $T'_\infty = 1400 \text{ }^\circ\text{K}$. The dissociation rates measured by Kewley & Hornung (1974) give $\epsilon = 2 \times 10^{-5}$ for flow over a 2 in. diameter cylinder, k'_0 being the shock curvature at the symmetry plane. The shock shape for such flows is well represented by the catenary $k = m$, so that $b = 3(1 - m^2)$. The experimental free stream is slightly dissociated, while the theory is derived for $\alpha_\infty = 0$. This may be accounted for in the theoretical results by evaluating $A_1(\xi_1)$ at the experimental value of ξ_1 , which may be obtained by substituting the experimental value of $\rho_1 = 5.5$ (see Hornung 1972, figure 13) in $\xi_1 = m^2(1 - \rho_1^{-1})/[\rho_1\theta(1 + \alpha_\infty)]$.

The interferogram is shown in figure 4 (plate 1). Superimposed on it are two curves. The full line is the locus of density maxima as determined from (7.5) and (7.6). The dashed line is the locus of points where streamlines (as calculated by a full numerical solution) are tangential to the experimental fringes. Since the streamline shapes are relatively insensitive to non-equilibrium effects, and since the refractive index of $\text{N}_2\text{-N}$ mixtures is only weakly affected by α , such points may be regarded as measurements of the positions of density maxima. It can be seen that the agreement between the measured and calculated locus of density maxima is quite good at the smaller values of ϕ but deteriorates rapidly as ϕ increases towards the symmetry plane. This occurs for two reasons. First, while (7.3) correctly predicts t_* to become very large as $m \rightarrow 1$, the approximation concerning v made to obtain y_* in (7.6) becomes very inaccurate as $m \rightarrow 1$. Second, throughout the analysis it has been assumed that $1 - m^2 = O(1)$, and terms $O(\delta)$ have been neglected by comparison. This assumption breaks down near the stagnation point and the theory becomes invalid there. Note that the recombination rate remains unimportant in this region, since (1.3) applies for the experimental flow. The discrepancy between the calculated and measured locus of density maxima at larger distances from the symmetry plane is partly due to the transverse curvature of the shock, which distorts the interferogram, particularly in the vicinity of the shock.

The transition from reacting to frozen flow may now be seen quite clearly: to the left of the locus of density maxima the fringe pattern is typical of reacting flow (fringes parallel to shock); to the right, or downstream, of it the pattern characterizes frozen flow (fringes approximately normal to body). The fact that the frozen region is different from a flow which is frozen throughout the field, in that a gradient of α exists across it, changes the fringe pattern in the frozen region in such a way that the fringes are slightly convex in the downstream direction, where in the fully frozen flow they would be concave. This is mainly a consequence of the dependence of ρ_0 on m .

To compare the calculated and measured values of the density maxima, $\rho_* - \rho_1$ is plotted against ϕ in figure 5 for the case of the experiment considered. The points are values calculated from the measured fringe shift and

$$\rho' - \rho'_\infty = \frac{4.16F\lambda'}{L'(1 + 0.28\alpha)} \text{ g cm}^{-3},$$

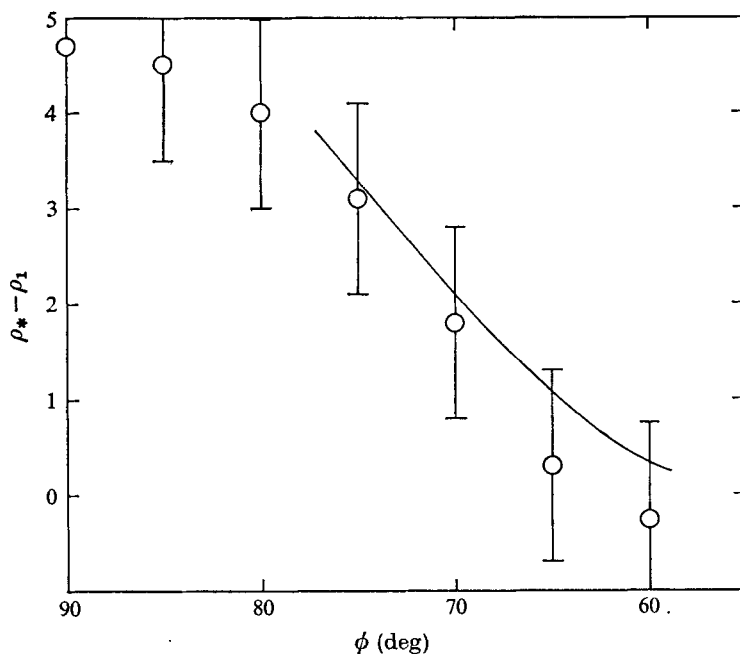


FIGURE 5. Value of the density increase at the maxima. \circ , measured, $\rho_1 = 5.5$; —, calculated from equation (7.4), $\rho_1 = 7$.

where (in this formula only) F is the fringe shift, λ' is the wavelength of the light used (533 nm) and L' is the geometric length of the optical path. The agreement is well within the experimental error.

One might now be tempted to use this understanding of blunt-body flow to determine the dependence of the dissociation rate on temperature from the variation of y_* with m . However, it is easy to see from (7.5), (7.6) and (7.8) that this is not satisfactory, because of the weak dependence of y_* on ϵ and the fact that the variation of y_* with m is a balance between the effect of the pressure gradient and temperature dependence of the rate.

8. Conclusions

Hypersonic flow after a curved shock with Lighthill-Freeman ideal-gas dissociation has been considered under circumstances such that the dissociation rate is fast and the recombination rate may be neglected.

It is shown that under these conditions the flow may be divided into two regions: a thin reacting layer near the shock, in which the effect of shock curvature is small, and a frozen-flow region further downstream. Analytic solutions are obtained for a streamline in the form of matched asymptotic expansions with the dissociation rate as a large parameter. If the thin reacting layer is considered to be part of the shock, effective shock conditions may be defined on each streamline for the frozen flow by extrapolating the frozen-flow solution back to the shock. The theory gives explicit expressions for these effective shock values.

The effective shock temperature for the frozen flow turns out to be practically independent of the shock slope and curvature. Hence the effective shock density varies with shock slope approximately like the effective shock pressure, namely like $m^2 = \sin^2 \phi$. This is in contrast to the situation for the shock values for a frozen flow, in which the density is independent of ϕ and the temperature varies as $\sin^2 \phi$.

An important result, which is also of interest in comparisons with experiment, is the distance from the shock of the density maximum on a streamline. This turns out to be proportional to

$$\sin^2 \phi / k \log (bc)^{-1}.$$

The fact that the logarithm appears in the denominator of the layer thickness is related to the exponential temperature dependence of the dissociation rate.

The results are shown to agree quite well with an experimental interferogram of nitrogen flow over a circular cylinder except in the vicinity of the symmetry plane, where the theory becomes invalid.

This work was supported by an Alexander von Humboldt fellowship at the Technische Hochschule Darmstadt. I wish to thank the Humboldt foundation for its generous support. It is with great pleasure that I thank Professor Becker and members of his group at the Institut für Mechanik for many discussions and for the pleasant surroundings provided for me. The interferogram was obtained in a shock tunnel financed by the Australian Research Grants Committee, whose support is gratefully acknowledged.

REFERENCES

- BECKER, E. & BÖHME, G. 1969 In *Nonequilibrium Flows. Part I* (ed. P. P. Wegener), p. 71. Marcell Dekker.
- FREEMAN, N. C. 1958 *J. Fluid Mech.* **4**, 407.
- FURLER, S. 1973 M.Sc. thesis, Australian National University, Canberra.
- HAYES, W. D. & PROBSTEIN, R. F. 1966 *Hypersonic Flow Theory*. Academic.
- HORNUNG, H. G. 1972 *J. Fluid Mech.* **53**, 149.
- KEWLEY, D. & HORNUNG, H. G. 1974 *Chem. Phys. Lett.* **25**, 531.
- LIGHTHILL, M. J. 1957 *J. Fluid Mech.* **2**, 1.
- VINCENTI, W. G. & KRUGER, C. H. 1965 *Introduction to Physical Gasdynamics*. Wiley.

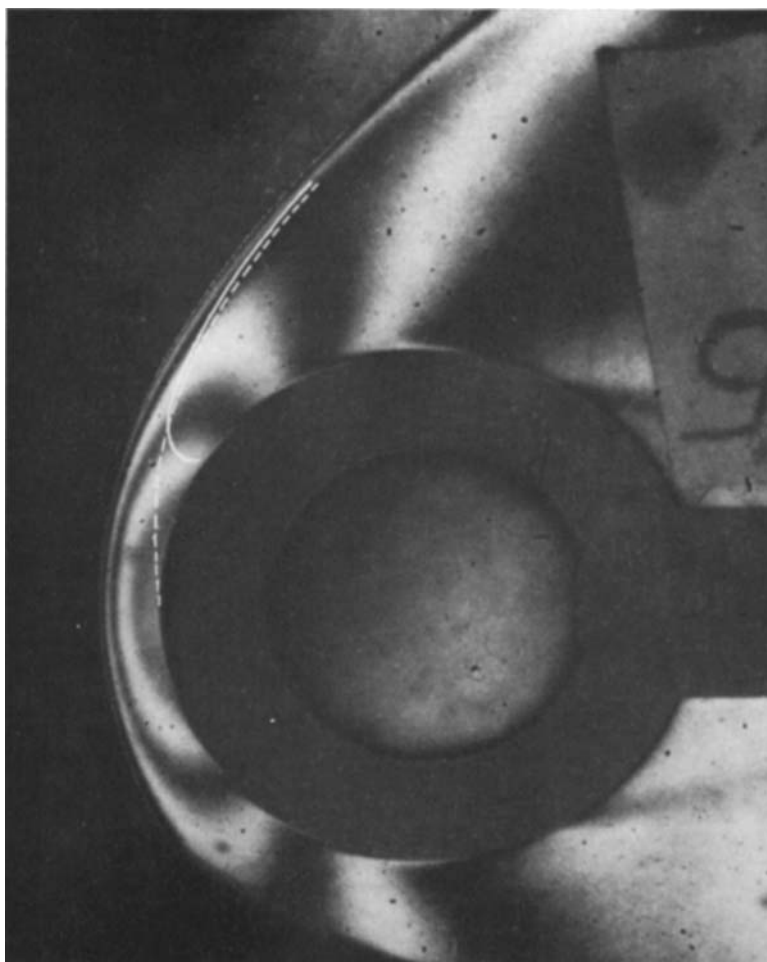


FIGURE 4. Comparison with experiment. Nitrogen flow over a 2 in. diameter circular cylinder. $V_{\infty}' = 5.5$ km/s, $\rho_{\infty} = 5.5$ g/cm³, $\alpha_{\infty} = 0.07$, $\theta = 0.92$, $T_{\infty}' = 1400$ °K, $\epsilon = 2 \times 10^{-5}$. —, locus of density maxima [equations (7.5), (7.6)]; ---, locus of density maxima from points of tangency of numerically calculated streamlines and measured interference fringes.